Second-Order Overtone and Combination Raman Modes of Graphene Layers in the Range of 1690−2150 cm^{-1}

Chunxiao Cong,[†] Ting Yu,[†,‡,*] Riichiro Saito,[§] Gene F. Dresselhaus,[⊥] and Mildred S. Dresselhaus[#,¶]

[†]Division of Physics and Applied Physics, School of Physical and Mathematical Sciences, Nanyang Technological University, 637371, Singapore, [‡]Department of Physics, Faculty of Science, National University of Singapore, 117542, Singapore, [§]Department of Physics, Tohoku University, Sendai, Miyagi 9808578, Japan, [⊥]Francis Bitter Magnet Laboratory, [#]Department of Electrical Engineering and Computer Science, and [¶]Department of Physics, Massachusetts Institute of Technology, Cambridge, Massachusetts 02139-4037, United States

ABSTRACT Though graphene has been intensively studied by Raman spectroscopy, in this letter, we report a study of the second-order overtone and combination Raman modes in a mostly unexplored frequency range of 1690−2150 cm^{-1} in nonsuspended commensurate (AB-stacked), incommensurate (folded) and suspended graphene layers. On the basis of the double resonance theory, four dominant modes in this range have been assigned to (i) the second order out-of-plane transverse mode (2oTO or M band), (ii) the combinational modes of in-plane transverse acoustic mode and longitudinal optical mode (iTA+LO), (iii) in-plane transverse optical mode and longitudinal acoustic mode (iTO+LA), and (iv) longitudinal optical mode and longitudinal acoustic mode (LO+LA). Differing from AB-stacked bilayer graphene or few layer graphene, single layer graphene shows the disappearance of the M band. Systematic analysis reveals that interlayer interaction is essential for the presence (or absence) of the M band, whereas the substrate has no effect on the presence (or absence) of the M band. Dispersive behaviors of these "new" Raman modes in graphene have been probed by laser excitation energy-dependent Raman spectroscopy. It is found that the appearance of the M band strictly depends on the AB stacking, which could be used as a fingerprint for AB-stacked bilayer graphene. This work expands upon the unique and powerful abilities of Raman spectroscopy to study graphene and provides another effective way to probe phonon dispersion, electron−phonon coupling, and to exploit the electronic band structure of graphene layers.

KEYWORDS: graphene · Raman · AB stacking · layer-dependence · electron−phonon coupling

Carbon materials occurring in many different forms, such as highly ordered pyrolytic graphite (HOPG), diamond, carbon fibers, carbon nanotubes, buckminsterfullerene, and so on, are very important for science and technology.[1,2] The recently discovered single layer graphene (SLG), which has unusual electronic properties, shows remarkable signs of applicability for fundamental studies and applications in nanoelectronics and nanophotonics.[3−5] Moreover, it was recently shown, both experimentally[6−8] and theoretically[9,10] that the electronic gap between the valence and conduction bands of AB-stacked bilayer graphene (BLG) can be controlled by an applied electric field. This makes BLG the only known semiconductor with a tunable energy gap and may open the way for developing photo detectors and lasers tunable by controlling the electric field.[6] Thus growing large area BLG is imperative for real applications and many researchers are devoting great efforts to this pursuit. Therefore, a fast accurate and nondestructive method, which can be used to distinguish AB-stacked BLG from other types of graphene is urgently needed.

In this work, we exploited the second-order overtone and combinational Raman modes in the range of 1690−2150 cm^{-1} of graphene layers, and we have identified all the dominant modes in this frequency range based on double resonance theory.[11,12] It is found that a band at about 1750 cm^{-1}, assigned as the M band, only appears in BLG or few layer graphene (FLG) and is absent in both SLG and incommensurate bilayer graphene (IBLG). This provides a fast and reliable way to distinguish BLG from SLG and IBLG, which should be very useful for future studies of BLG and the development of nanodevices based on BLG.

As exploited by previous experimental and theoretical studies, the novel properties of graphene layers are due to their unique electronic band structures. Understanding the behavior of electrons and phonons in graphene layers is also very important for their practical applications in electronic devices. Raman spectra provide precise information on the crystal structure, electronic band structure, the phonon energy dispersion,

*Address correspondence to yuting@ntu.edu.sg.

Received for review October 26, 2010 and accepted January 25, 2011.

Published online February 23, 2011
10.1021/nn200010m

and the electron−phonon interaction in sp^2 carbon systems.[13,14] It has been shown experimentally that by monitoring the position, width, integrated intensity, and line shape of the Raman features of the graphene layers, the number of their layers,[15,16] the linear dispersion of their electronic energy,[17] the crystal orientation,[18−20] the doping,[21,22] the defects,[23] strain,[24,25] and the thermal conductivity[26−28] can all be probed. The most prominent peaks in the Raman spectrum of graphene layers are the so-called G mode and G′ (or 2D) mode, which are associated with the doubly degenerate in-plane transverse optical phonon mode and longitudinal optical phonon mode (iTO and LO) at the Γ point and with an intervalley double resonance process involving two iTO phonons near the K point, respectively. If a laser beam is focused on the edges of graphene or if some defects exist, two additional peaks will appear, named the D mode and the D′ mode, which are, respectively, due to an intervalley double resonance process involving defects and iTO phonons and an intravalley double resonance process involving defects and LO phonons. To our knowledge, Raman features in the range of 1690−2150 cm^{-1} in graphene layers were never reported previously, though they have been studied in single wall carbon nanotubes (SWNTs),[29,30] and in highly ordered pyrolytic graphite (HOPG),[29] graphite whiskers,[31] double wall carbon nanotubes (DWCNTs),[32] and multiwall carbon nanotubes (MWNTs).[33] Our work presented in this letter discloses the nature of these modes. The energy dependence of the combination modes in this frequency range is given through a detailed laser excitation-energy-dependent Raman spectroscopy study.

RESULTS AND DISCUSSION

The electronic and vibrational properties of graphene layers could be significantly different when their thicknesses or number of layers are varied. Several techniques have been adapted for identifying the number of layers of graphene films, such as the quantum Hall effect,[4,5] atomic force microscopy (AFM),[5] transmission electron microscopy (TEM),[34] Raman spectroscopy,[15] and contrast spectroscopy[16] measurements, *etc*. Among them, the optical approaches such as Raman and contrast spectroscopy are most favorable because of their unique advantages such as non-destructive, no sample preparation requirement, and fast processing. Figure 1a shows the optical images of selected graphene layers. The white light contrast spectra of the selected graphene layers are shown in Figure 1b. By using the method reported in ref 16, the number of layers of these graphene films is determined from one to seven, as labeled in the optical images of Figure 1. The extracted contrast values as a function of the number of layers shown in Figure 1c are also in agreement with the results in ref 16. To doubly confirm the number of layers, Raman spectra of these graphene films were recorded and fitted.

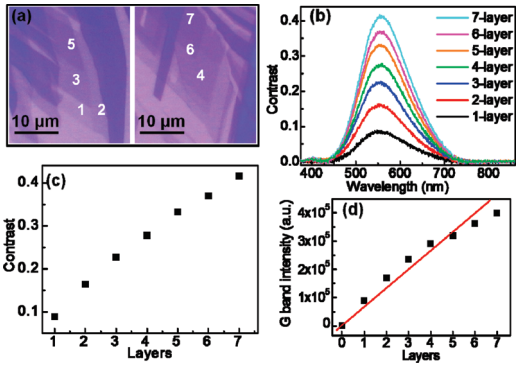

Figure 1. (a) Optical images of selected graphene films with different numbers of layers. (b) The contrast spectra of the selected graphene films as indicated in panel a. (c) The contrast values extracted from panel b as a function of number of layers. (d) G band absolute integrated intensity of graphene films measured under the same conditions as panel b.

Figure 1d presents the Raman G band intensity as a function of the number of layers. The nearly linear dependence could be another method for layer number determination.[35] The width of the G′ mode was also measured to identify the number of layers of graphene films.[15]

Graphene has been intensively studied by Raman spectroscopy, but very little attention was afforded to the spectral range between 1690 and 2150 cm^{-1}, where several modes have actually been observed in other graphitic materials like carbon nanotubes, graphite, and graphite whiskers. Equally importantly and interestingly, these modes also result from the double resonance process and carry information on the electron−favorable because of their unique advantages such as non-destructive, no sample preparation requirement, and fast processing.phonon coupling. Figure 2a presents typical Raman spectra for SLG and BLG; in addition to the strong G and G′ peaks, some weak peaks existing between 1690 and 2150 cm^{-1} are seen. Figure 2 panels b and c show the Raman spectra of various numbers of graphene layers (1 to 7 layers) in this range together with the spectrum of HOPG. For comparison, the G′ mode is also shown in Figure 2d. Similarly, but much more obviously compared to the G′ mode, the Raman modes between 1690 and 2150 cm^{-1} display an evolution of the spectral components, such as line-shape, peak position, and peak width with increasing numbers of layers.

To reveal the nature of these modes within this almost unexplored range, we divide the modes into two groups. One is in the range 1690−1800 cm^{-1} (Figure 2b) and the other is in the range 1800−2150 cm^{-1} (Figure 2c), which correspond, respectively, to the M band range and the combination mode range as discussed previously for SWNTs.[29] In the M band range, the most remarkable observation in Figure 2b is the absence of any peak in the spectrum of SLG, whereas the BLG and FLG show two obvious peaks with multiple components. These spectral features clearly differ from the G′ mode, which shows asymmetry and broadening with increasing layer numbers, due to the extra components introduced by the

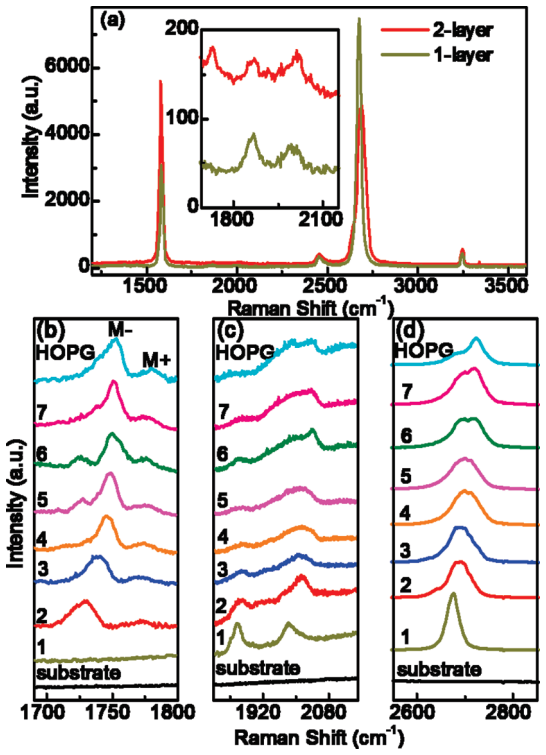

Figure 2. (a) Raman spectra of 1-layer and 2-layer graphene on a 300 nm SiO_2/Si substrate. The inset shows zoom-in spectra in the range of 1690−2150 cm^{-1}. Panels b, c, and d are the Raman spectra of a 300 nm SiO_2/Si substrate, graphene sheets with different numbers of layers, and HOPG, all supported on the 300 nm SiO_2/Si substrate in the frequency ranges of interest 1690−1800 cm^{-1}, 1800−2150 cm^{-1}, and 2550−2850 cm^{-1}, respectively.

existence of extra electronic branches in BLG and FLG, while only one sharp and strong peak appears in the spectrum of SLG. This distinguishable behavior of the modes in the M band range and the G′ mode could be explained by the physical processes responsible for their origins. The G′ mode or the overtone of the iTO mode is Raman active for all numbers of graphene layers. In contrast, the M band is the overtone of the oTO phonon, an infrared-active out-of-plane mode. For SWNTs due to the confinement (zone folding) effects and for HOPG due to the interlayer coupling, the Raman mode selection rules could be relaxed and this oTO mode would become Raman active. In the case of SWNTs, depending on the energy of the van Hove singularity relative to the laser excitation energy, the M band could selectively appear in carbon nanotubes of certain chiralities (n, m) and diameters.[36] Furthermore, for SWNTs, various line-shapes and a step-like phonon dispersion of such intermediate frequency modes could be also the result from this (n, m) dependence.[37] On the other hand, for HOPG, FLG, and BLG, there is no such special resonance effect associated with van Hove singularities. The resonance condition for these two dimensional structures can always be satisfied. The nonzone-center phonons connected with the Γ point, as reflected by this oTO mode, undergo an electron double resonant intravalley scattering in possible ways, one with a near-zero momentum, appearing as the M^+ band, and the other with a momentum that is the double that of the scattered excited electrons, named the M^- band (indicated in Figure 2b).[29] Considering the above findings, we attribute the phonon mode of the BLG and FLG in the range of 1690−1800 cm^{-1} to the M band caused by an intravalley double resonance scattering process. Similar to the G′ mode, the evolution of this M band with an increase in the number of layers might be mainly due to the evolution of the electronic band structure of graphene films. The existence of this M band could be a fingerprint of the AB stacking in BLG. More discussion of this point is given below.

The evolution of the modes with increasing number of graphene layers could be also observed in the Raman spectra in the combination mode range between 1800 and 2150 cm^{-1} as shown in Figure 2c. Several arguments about the assignments of the Raman modes of carbon materials in this range were reported in previous studies. For example, in HOPG (SWNTs), the peak at 1950 cm^{-1} (1987 cm^{-1}) was tentatively assigned as a combination of the in-plane transverse optic (iTO) and longitudinal acoustic (LA) modes (iTO+LA) in 2002.[29] Another group later claimed that this asymmetric peak consists of two modes, named iTO+LA and LO+LA.[30] For graphite whiskers, the two peaks in this range were identified as iTA+LO and LO+LA.[31] However, no conclusive assignments are yet available, especially for graphene. With careful curve fitting and systematic analysis, we believe there are three dominant peaks in this combination mode range, as seen in Figure 2.

Figure 3a shows the Raman spectra of the SLG in the combinational mode range taken with various laser excitation energies. All the peaks display a blue-shift with increasing laser excitation energy, which was also observed in previous measurements[29,38] and can be understood by double resonance theory.[11,12] To exploit these details, the experimental data were fitted by three Lorentzian line shape peaks and the fitting curves match the experimental data very well. The frequencies of these modes are plotted in Figure 3b as a function of the laser excitation energies. A positive and linear laser excitation energy dependence of these phonons is clearly seen in Figure 3b, which indicates that the origin of these peaks come from a double resonance process, the same as describes the well-studied D and G′ modes. To fulfill the double resonance Raman process, the momentum of the phonon must be nearly twice that of the intravalley or intervalley scattered electrons. In SLG, at a relative low energy level (<3 eV), the electronic spectrum is linear near the K point. Therefore, the electron energy shows a linear dependence on phonon momentum, which promises Raman spectroscopy to be a unique and powerful tool for probing both the electronic structure and the phonon dispersion of graphene. Benefiting from this linear dependence, we depict the phonon dispersion frequency *versus* phonon wave vector in Figure 3b (top scale). The energy dependence (the slope) of

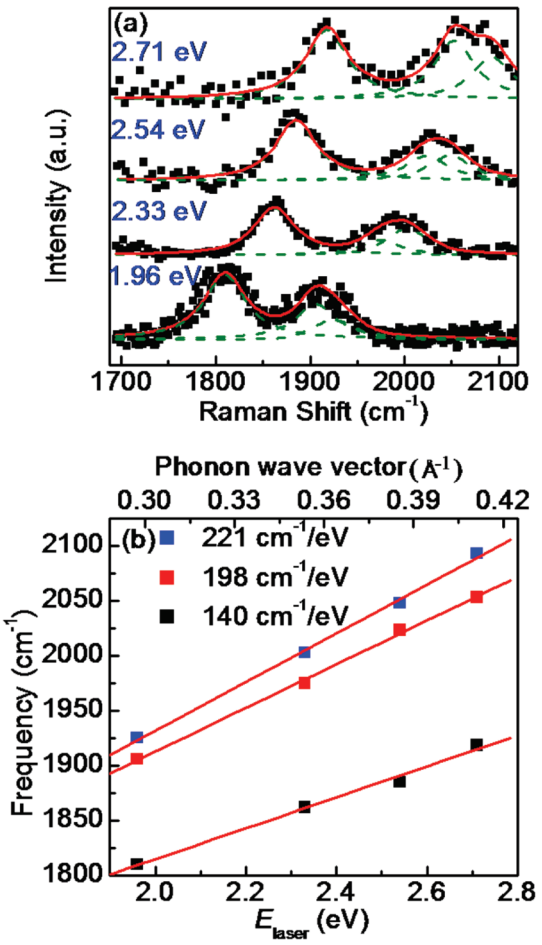

Figure 3. (a) Raman spectra taken at several E_{laser} values for SLG in the combination mode range. (b) Plot of the resulting peak frequencies as a function of E_{laser} (bottom scale) and of the phonon wave vector (top scale).

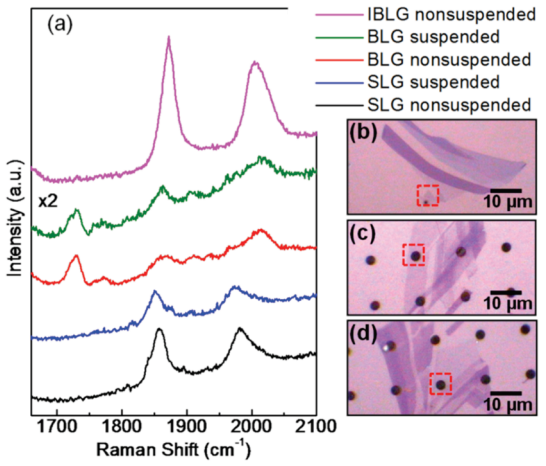

Figure 4. (a) Raman spectra of the suspended SLG and BLG, and the nonsuspended SLG, BLG, and the incommensurate BLG (IBLG). (b) Optical image of the incommensurate BLG on a 300 nm SiO_2/Si substrate. (c, d) Optical images of graphene sheets on a patterned 300 nm SiO_2/Si substrate covering holes. The incommensurate BLG, the suspended BLG, and the suspended SLG were marked by red dash-line square on panels b, c, and d, respectively.

these three peaks is estimated to be 140 cm^{-1}/eV for the lowest frequency mode, 198 cm^{-1}/eV for the medium frequency, and 221 cm^{-1}/eV for the highest frequency mode. For the 532 nm laser (excitation energy of 2.33 eV), the lowest frequency mode is located at 1860 cm^{-1}, which very well matches the combination of iTA and iTO. (Our readings from the dispersion curve in ref 29 are that $\omega_{iTA} = 300$ cm^{-1} and $\omega_{iTO} = 1560$ cm^{-1} for 2.33 eV). However, the frequency of a combination mode is usually a bit less than the sum frequency of the mother-components.[31] Moreover, the energy dependence or the slope of the dispersion curve of the iTA mode is 129 cm^{-1}/eV,[31] and the iTO mode shows a negative dispersion in the range studied in this work, which cannot lead to a mode with an energy dependence of 140 cm^{-1}/eV by combining these two modes (iTA+iTO). In contrast to the iTO mode, the LO mode disperses positively within this range and is located at 1600 cm^{-1} for the 2.33 eV laser. Therefore, the iTA+LO could be responsible for this low frequency peak. This assignment could also be supported by the study on graphite whiskers, where an energy dependence of 139 cm^{-1}/eV was observed for an iTA+LO mode.[31] This very good "agreement" may hint that SLG may share some structural features in common with graphite whiskers. Following the same strategy and considering the findings that the energy dependence of the LA mode is 216 cm^{-1}/eV,[31] the medium frequency mode with an energy dependence of 198 cm^{-1}/eV is attributed to a combination of iTO (with a negative energy dependence) and LA, while the high frequency mode with an energy dependence of 221 cm^{-1}/eV is attributed to a combination of LO (with a positive energy dependence) and LA. This agrees with the work on SWNTs[30] and could explain why the peak shows an asymmetric line shape in ref 31, which actually consists of two combinational modes: iTO+LA and LO+LA.

As a single atomic layer, graphene is extremely sensitive to the substrates, which is clearly reflected in their Raman spectra.[39] To investigate the substrate effects on the Raman spectra of graphene in the range of 1690 and 2150 cm^{-1}, non-suspended and suspended SLG and BLG samples were prepared, and the corresponding spectra are shown in Figure 4a. From these spectra, it can be clearly seen that the substrate has no significant effect on the frequency of the M band and on the combination modes of SLG and BLG. Further analysis of the interlayer coupling was performed on the Raman spectrum of the IBLG sample. Similar to the G′ mode, the integrated intensity of the combination modes is dramatically increased in such IBLG, and a blue-shift is observed, which is due to the reduction of charging impurities[39] and of the Fermi velocity,[40] respectively. The most significant and meaningful observation is the effect of the twisting of the two layers or the breaking of the AB (Bernal) stacking order which totally suppresses the M band as shown in the Raman spectrum of IBLG (see Figure 4). This might be due to the breaking of the stacking order of the A and B

sublattices in the two layers and consequently the oTO mode becomes a non-Raman active mode. The IBLG sample is more like two "isolated" SLGs. A detailed theoretical study is needed to exploit the interlayer coupling effects on this M band. The missing M band could be also observed in the Raman spectrum of the graphite whisker, which is similar to disordered graphite or to thick incommensurate graphene layers,[31] once again, indicating the commonalities among graphite whiskers, IBLG, and SLG. The absence of the M band in the IBLG Raman spectra makes the M band a unique feature for distinguishing AB-stacked BLG, indicating the potential use of this M band for practical applications.

CONCLUSION

We have studied the second order overtone and combination Raman modes of graphene layers in the virtually unexplored phonon frequency range of 1690−2150 cm^{-1}. All the dominant modes in this range have been assigned based on the double resonance Raman process. The energy dependences of the combination modes in the visible range have been obtained from the laser excitation-energy-dependent Raman spectra. The M band, which is strictly related to the AB stacking, provides a fast and accurate way to distinguish BLG from SLG and IBLG. All the modes in this range show a clear layer dependent evolution, which should be related to the changes of the electronic structures of few layer graphene. The results herein clearly demonstrate the unique and new potential of Raman scattering for probing the graphene electronic band structure, the phonon energy dispersion, and the electron−phonon interaction in few-layer graphene as a function of layer numbers.

EXPERIMENTAL METHODS

In this work, nonsuspendend commensurate (AB-stacked), incommensurate (folded), and suspended graphene layers were studied. The graphene layers were prepared by mechanical cleavage of HOPG and transferred onto a 300 nm SiO_2/Si substrate. The majority of the transferred graphene layers are AB-stacked, whereas some parts of the SLG may fold over during the transfer and form incommensurate BLG.[41] The detailed process of fabrication suspended samples is described in ref 39. In general, a 300 nm SiO_2/Si substrate with prepatterned holes was used. After transfer, some parts of the graphene layers covering the holes are suspended. An optical microscope was used to locate the thin layers, and the number of layers was further identified by white light contrast spectra, the width of the G′ mode, and the absolute Raman intensity of the G mode. The white light contrast spectra were acquired using a WITec CRM200 Raman system with a 150 lines/mm grating. The Raman spectra were obtained using a Renishaw system with a 2400 lines/mm grating and using a 532 nm laser (E_{laser} = 2.33 eV) excitation. The laser excitation-energy-dependent Raman spectra were recorded using a WITec CRM200 Raman system with a 600 lines/mm grating. The laser power was kept below 0.1 mW on the sample surface to avoid laser-induced heating.

Acknowledgment. This work is supported by the Singapore National Research Foundation under NRF RF Award No. NRF-RF2010-07 and MOE Tier 2 MOE2009-T2-1-037. C. Cong thanks Professor T. Enoki for his enlightening discussions. R. Saito acknowledges MEXT Grant No. 20241023. M. Dresselhaus and G. Dresselhaus acknowledge NSF/DMR 10-04147.

REFERENCES AND NOTES

1. Dresselhaus, M. S.; Dresselhaus, G.; Sugihara, K.; Spain, I. L.; Goldberg, H. A. *Graphite Fibers and Filaments*; Springer Series in Materials Science, Vol. 5; Springer-Verlag: Berlin, 1988.
2. Olle Ingan; Ingemar Lundst Carbon Nanotube Muscles. *Science* 1999, *284*, 1281-1282.
3. Novoselov, K. S.; Geim, A. K.; Morozov, S. V.; Jiang, D.; Zhang, Y.; Dubonos, S. V.; Grigorieva, I. V.; Firsov, A. A. Electric Field Effect in Atomically Thin Carbon Films. *Science* **2004,** *306*, 666–669.
4. Novoselov, K. S.; Geim, A. K.; Morozov, S. V.; Jiang, D.; Katsnelson, M. I.; Grigorieva, I. V.; Dubonos, S. V.; Firsov, A. A. Two-dimensional Gas of Massless Dirac Fermions in Graphene. *Nature* **2005,** *438*, 197–200.
5. Zhang, Y.; Tan, Y. W.; Stormer, H. L.; Kim, P. Experimental Observation of the Quantum Hall Effect and Berry's Phase in Graphene. *Nature* **2005,** *438*, 201–204.
6. Castro, E. V.; Novoselov, K. S.; Morozov, S. V.; Peres, N. M. R.; Lopes dos Santos, J. M. B.; Nilsson, J.; Guinea, F.; Geim, A. K.; Castro Neto, A. H. Biased Bilayer Graphene: Semiconductor with a Gap Tunable by the Electric Field Effect. *Phys. Rev. Lett.* **2007,** *99*, 216802-1–216802-4.
7. Oostinga, J. B.; Heersche, H. B.; Liu, X.; Morpurgo, A. F.; Vandersypen, L. M. K. Gate-Induced Insulating State in Bilayer Graphene Devices. *Nat. Mater.* **2007,** *7*, 151–157.
8. Zhang, Y.; Tang, T.-T.; Girit, C.; Hao, Z.; Martin, M. C.; Zettl, A.; Crommie, M. F.; Shen, Y. R.; Wang, F. Direct Observation of a Widely Tunable Bandgap in Bilayer Graphene. *Nature* **2009,** *459*, 820–823.
9. McCann, E. Asymmetry Gap in the Electronic Band Structure of Bilayer Graphene. *Phys. Rev. B* **2006,** *74*, 161403(R)–161406(R).
10. Min, H.; Sahu, B.; Banerjee, S. K.; MacDonald, A. H. *Ab Initio* Theory of Gate Induced Gaps in Graphene Bilayers. *Phys. Rev. B* **2007,** *75*, 155115–155121.
11. Thomsen, C.; Reich, S. Double Resonant Raman Scattering in Graphite. *Phys. Rev. Lett.* **2000,** *85*, 5214–5217.
12. Saito, R.; Jorio, A.; Souza Filho, A. G.; Dresselhaus, G.; Dresselhaus, M. S.; Pimenta, M. A. Probing Phonon Dispersion Relations of Graphite by Double Resonance Raman Scattering. *Phys. Rev. Lett.* **2002,** *88*, 027401−1–027401−4.
13. Dresselhaus, M. S.; Jorio, A.; Saito, R. Characterizing Graphene, Graphite, and Carbon Nanotubes by Raman Spectroscopy. *Annu. Rev. Condens. Matter Phys.* **2010,** *1*, 89–108.
14. Jorio, A.; Dresselhaus, M. S.; Saito, R. Dresselhaus, G. F. *Raman Spectroscopy in Graphene Related Systems*; Wiley-VCH: Berlin, 2011.
15. Ferrari, A. C.; Meyer, J. C.; Scardaci, V.; Casiraghi, C.; Lazzeri, M.; Mauri, F.; Piscanec, S.; Jiang, D.; Novoselov, K. S.; Roth, S.; *et al.* Raman Spectrum of Graphene and Graphene Layers. *Phys. Rev. Lett.* **2006,** *97*, 187401−1–187401−4.
16. Ni, Z. H.; Wang, H. M.; Kasim, J.; Fan, H. M.; Yu, T.; Wu, Y. H.; Feng, Y. P.; Shen, Z. X. Graphene Thickness Determination Using Reflection and Contrast Spectroscopy. *Nano Lett.* **2007,** *7*, 2758–2763.
17. Mafra, D. L.; Samsonidze, G.; Malard, L. M.; Elias, D. C.; Brant, J. C.; Plentz, F.; Alves, E. S.; Pimenta, M. A. Determination of LA and TO Phonon Dispersion Relations of Graphene Near the Dirac Point by Double Resonance Raman Scattering. *Phys. Rev. B* **2007,** *76*, 233407−1–233407−4.
18. Huang, M.; Yan, H.; Chen, C.; Song, D.; Heinz, T. F.; Hone, J. Phonon Softening and Crystallographic Orientation of

Strained Graphene Studied by Raman Spectroscopy. *Proc. Natl. Acad. Sci. U.S.A.* **2009,** *106*, 7304–7308.
19. Mohiuddin, T. M. G.; Lombardo, A.; Nair, R. R.; Bonetti, A.; Savini, G.; Jalil, R.; Bonini, N.; Basko, D. M.; Galiotis, C.; Marzari, N.; *et al.* Uniaxial Strain in Graphene by Raman Spectroscopy: G Peak Splitting, Grüneisen Parameters, and Sample Orientation. *Phys. Rev. B* **2007,** *79*, 205433−1–205433−8.
20. You, Y. M.; Ni, Z. H.; Yu, T.; Shen, Z. X. Edge Chirality Determination of Graphene by Raman Spectroscopy. *Appl. Phys. Lett.* **2008,** *93*, 163112−1–163112−3.
21. Das, A.; Pisana, S.; Chakraborty, B.; Piscanec, S.; Saha, S. K.; Waghmare, U. V.; Novoselov, K. S.; Krishnamurthy, H. R.; Geim, A. K.; Ferrari, A. C.; *et al.* Monitoring Dopants by Raman Scattering in an Electrochemically Top-Gated Graphene Transistor. *Nat. Nanotechnol.* **2008,** *3*, 210–215.
22. Luo, Z.; Yu, T; Kim, K.; Ni, Z.; You, Y.; Lim, S.; Shen, Z.; Wang, S.; Lin, J. Thickness-Dependent Reversible Hydrogenation of Graphene Layers. *ACS Nano* **2009,** *3*, 1781–1788.
23. Cancado, L. G.; Pimenta, M. A.; Saito, R.; Jorio, A.; Ladeira, L. O.; Grueneis, A.; Souza-Filho, A. G.; Dresselhaus, G.; Dresselhaus, M. S. Stokes and Anti-Stokes Double Resonance Raman Scattering in Two-Dimensional Graphite. *Phys. Rev. B* **2002,** *66*, 035415−1–035415−5.
24. Yu, T.; Ni, Z.; Du, C.; You, Y.; Wang, Y.; Shen, Z. Raman Mapping Investigation of Graphene on Transparent Flexible Substrate: The Strain Effect. *J. Phys. Chem. C* **2008,** *112*, 12602–12605.
25. Ni, Z. H.; Yu, T.; Lu, Y. H.; Wang, Y. Y.; Feng, Y. P.; Shen, Z. X. Uniaxial Strain on Graphene: Raman Spectroscopy Study and Band-Gap Opening. *ACS Nano* **2008,** *2*, 2301–2305.
26. Ghosh, S.; Calizo, I.; Teweldebrhan, D.; Pokatilov, E. P.; Nika, D. L.; Balandin, A. A.; Bao, W.; Miao, F.; Lau, C. N. Extremely High Thermal Conductivity of Graphene: Prospects for Thermal Management Applications in Nanoelectronic Circuits. *Appl. Phys. Lett.* **2008,** *92*, 151911−1–151911−3.
27. Balandin, A. A.; Ghosh, S.; Bao, W.; Calizo, I.; Teweldebrhan, D.; Miao, F.; Lau, C. N. Superior Thermal Conductivity of Single-Layer Graphene. *Nano Lett.* **2008,** *8*, 902–907.
28. Ghosh, S.; Bao, W.; Nika, D. L.; Subrina, S.; Pokatilov, E. P.; Lau, C. N.; Balandin, A. A. Dimensional Crossover of Thermal Transport in Few-Layer Graphene. *Nat. Mater.* **2010,** *9*, 555–558.
29. Brar, V. W.; Samsonidze, Ge. G.; Dresselhaus, M. S.; Dresselhaus, G.; Saito, R.; Swan, A. K.; Unl ü, M. S.; Goldberg, B. B.; Souza Filho, A. G.; Jorio, A. Second-Order Harmonic and Combination Modes in Graphite, Single-Wall Carbon Nanotube Bundles, and Isolated Single-Wall Carbon Nanotubes. *Phys. Rev. B* **2002,** *66*, 155418–155427.
30. Fantini, C.; Pimenta, M. A.; Strano, M. S. Two-Phonon Combination Raman Modes in Covalently Functionalized Single-Wall Carbon Nanotubes. *J. Phys. Chem. C* **2008,** *112*, 13150–13155.
31. Tan, P. H.; Dimovski, S.; Gogotsi, Y. Raman Scattering of Non-planar Graphite: Arched Edges, Polyhedral Crystals, Whiskers, and Cones. *Phil. Trans. R. Soc. London, A* **2004,** *362*, 2289–2310.
32. Ellis, A. V. Second-Order Overtone and Combination Modes in the LOLA Region of Acid-Treated Double-Walled Carbon Nanotubes. *J. Chem. Phys.* **2006,** *125*, 121103−1–121103−5.
33. Tan, P. H.; An, L.; Liu, L. Q.; Guo, Z. X.; Czerw, R.; Carrol, D. L.; Ajayan, P. M.; Zhang, N.; Guo, H. L. Probing the Phonon Dispersion Relations of Graphite from the Double-Resonance Process of Stokes and Anti-Stokes Raman Scatterings in Multiwalled Carbon Nanotubes. *Phys. Rev. B* **2002,** *66*, 245410−1–245410−8.
34. Meyer, Jannik C.; Geim, A. K.; Katsnelson, M. I.; Novoselov, K. S.; Booth, T. J.; Roth, S. The Structure of Suspended Graphene Sheets. *Nature* **2007,** *446*, 60–63.
35. Graf, D.; Molitor, F.; Ensslin, K.; Stampfer, C.; Jungen, A.; Hierold, C.; Wirtz, L. Spatially Resolved Raman Spectroscopy of Single- and Few-Layer Graphene. *Nano Lett.* **2007,** *7*, 238–242.
36. Samsonidze, Ge. G.; Saito, R.; Jorio, a.; Souza Filho, A. G.; Grüneis, A.; Pimenta, M. A.; Dresselhaus, G.; Dresslhaus, M. S. Phonon Trigonal Warping Effect in Graphite and Carbon Nanotubes. *Phys. Rev. Lett.* **2003,** *90*, 027403−1–027403−4.
37. Fantini, C.; Jorio, A.; Souza, M.; Saito, R.; Samsonidze, Ge. G.; Dresselhaus, M. S.; Pimenta, M. A. Steplike Dispersion of the Intermediate-Frequency Raman Modes in Semiconducting and Metallic Carbon Nanotubes. *Phys. Rev. B* **2005,** *72*, 085446−1–085446−5.
38. Calizo, I.; Bejenari, I.; Rahman, M.; Liu, G.; Balandin, A. A. Ultraviolet Raman Microscopy of Single and Multilayer Graphene. *J. Appl. Phys.* **2009,** *106*, 043509-1–043509-5.
39. Ni, Z. H.; Yu, T.; Luo, Z. Q.; Wang, Y. Y.; Liu, L.; Wong, C. P.; Miao, J.; Huang, W.; Shen, Z. X. Probing Charged Impurities in Suspended Graphene Using Raman Spectroscopy. *ACS Nano* **2009,** *3*, 569–574.
40. Ni, Z. H.; Wang, Y. Y; Yu, T.; You, Y. M.; Shen, Z. X. Reduction of Fermi Velocity in Folded Graphene Observed by Resonance Raman Spectroscopy. *Phys. Rev. B* **2008,** *77*, 235403−1–235403−5.
41. Ni, Z. H.; Liu, L.; Wang, Y. Y.; Zheng, Z.; Li, L.-J.; Yu, T.; Shen, Z. X. G-band Raman Double Resonance in Twisted Bilayer Graphene: Evidence of Band Splitting and Folding. *Phys. Rev. B* **2009,** *80*, 125404-1–125404-5.